



Synthesis, characterization and antitumor activity of palladium(II) complexes of imidazolidine-2-thione

Thales R. de Moura¹  · Sahra L. Cavalcanti¹ · Paulo R. D. V. de Godoy² · Elza T. Sakamoto-Hojo² · Fillipe V. Rocha³ · Eduardo T. de Almeida⁴ · Victor M. Deflon⁵ · Antonio E. Mauro¹ · Adelino V. G. Netto¹ 

Received: 27 March 2017 / Accepted: 28 June 2017 / Published online: 11 July 2017
© Springer International Publishing AG 2017

Abstract Complexes of the type *cis*-[PdX₂(imzt)(PPh₃)] {imzt = imidazolidine-2-thione; PPh₃ = triphenylphosphine; X = Cl (**1**), Br (**2**), I (**3**), SCN (**4**)} have been synthesized and characterized by elemental analyses, molar conductance, IR and ¹H NMR spectroscopies. The complex **1**·MeOH was obtained from the reaction of [PdCl₂(CH₃CN)₂], imidazolidine-2-thione and triphenylphosphine in CHCl₃/CH₃OH. Complexes **2**·MeOH, **3** and **4** were prepared by metathesis of the chlorido ligands in **1** with bromide, iodide and thiocyanate, respectively. Elemental analyses showed good agreement with the expected mononuclear compositions, while the molar conductivities of the complexes in DMF were consistent with their non-electrolytic nature. NMR spectra confirmed coordination of

the imidazolidine-2-thione and triphenylphosphine ligands. Single-crystal X-ray diffraction determination of **1**·CH₃OH showed that the coordination geometry around Pd^{II} is nearly square planar, with the chlorido ligands in a *cis* configuration. All four complexes have been tested in vitro by XTT assay for their cytotoxicity against human glioblastoma cell line (U87MG). The binding of **1** with guanosine was studied by ¹H NMR spectroscopy, revealing that the coordination takes place via N7.

Introduction

Gliomas are the most commonly occurring form of brain tumor. Particularly, glioblastoma multiforme (GBM) is the most malignant and severe type of brain tumor, with a high proliferation rate and low survival rates in comparison with all human cancers [1, 2]. Despite its limited success, temozolomide (TMZ) is the first line drug employed in the treatment of brain cancer [3]. Platinum compounds (cisplatin, carboplatin and oxaliplatin) are also used in association with TMZ to treat recurrent glioma [4]. Single-agent carboplatin/cisplatin has modest activity in patients with recurrent HGG previously treated with one line of chemotherapy, nitrosoureas or temozolomide [5]. However, their use has several limitations including nephrotoxicity, irreversible neurotoxicity and intrinsic/acquired resistance [6]. Therefore, the poor prognosis associated with these tumors together with limitations of current therapies has demanded intensive efforts to develop more effective drugs with lower toxicity and improved therapeutic properties.

In an effort to generate novel metal-based compounds that overcome the limitations associated with the use of

Electronic supplementary material The online version of this article (doi:10.1007/s11243-017-0161-9) contains supplementary material, which is available to authorized users.

✉ Thales R. de Moura
thales4014@gmail.com

✉ Adelino V. G. Netto
adelino@iq.unesp.br

- ¹ Departamento de Química Geral e Inorgânica, Instituto de Química de Araraquara, UNESP – Univ Estadual Paulista, P.O. Box 355, Araraquara, São Paulo 14801–970, Brazil
- ² Departamento de Biologia, Faculdade de Filosofia, Ciências e Letras de Ribeirão Preto, USP Av. Bandeirantes 3900, Ribeirão Preto, São Paulo 14040-901, Brazil
- ³ Departamento de Química, Universidade Federal de São Carlos, São Carlos, São Paulo CEP 13.565-905, Brazil
- ⁴ Instituto de Química, UNIFAL - MG - Univ Federal de Alfenas, Alfenas, Minas Gerais 37130-000, Brazil
- ⁵ Instituto de Química de São Carlos, Universidade de São Paulo, Avenida Trabalhador São-carlense, 400, São Carlos, São Paulo CEP 13566-590, Brazil

platinum-based drugs in current clinical treatments, complexes containing different transition metals combined with a variety of ligand classes have been prepared and evaluated against cancer cell lines [7]. In this context, palladium(II) derivatives have emerged as potential alternative candidates for new metal antitumor drugs due to their structural and thermodynamic similarities to platinum(II) complexes [8]. In this context, phosphine ligands have been widely employed to design new bioactive complexes. Many authors have proposed that the incorporation of phosphine ligands into palladium(II) complexes results in an increase of cytotoxicity by enhancing the lipid solubility of the complex, hence providing better membrane penetration [9]. In addition, the bulkiness of these ligands is expected to decrease the rate of associative substitution reactions, which may increase the kinetic stability of these complexes in biological media [9]. For instance, mononuclear organometallic compounds bearing diphosphines [PdN₃(C-dmba)(dppp)] and [Pd(C²,N-dmba)(dppet)(N₃) (dmba = *N,N*-dimethylbenzylamine; dppp = 1,3-bis(diphenylphosphino)propane; dppet = *cis*-1,2-bis(diphenylphosphino)ethylene) displayed promising cytotoxicity against glioblastoma C6 cell line, with IC₅₀ values less than 1 μM [10].

In particular, compounds bearing the “Pd(S)(PR₃)” core (S = sulfur-donor ligand; PR₃ = monodentate phosphine) exhibited promising cytotoxic effects toward some human cancer cell lines as well as some pathogenic microbes [11]. In this context, complexes with general formula [Pd(L)₂(PPh₃)₂]Cl₂ and [Pd(L)₂(PPh₃)₂] (L = thiourea or heterocyclic thioamide; PPh₃ = triphenylphosphine) were developed by Nadeem et al. [11], and screened for cytotoxic activity with encouraging *in vitro* results against prostate cancer cells (PC3).

Motivated by the aforementioned observations, and as a part of our continuing research program in the field of coordination and biological chemistry of metal complexes [12–19], we present herein the synthesis and characterization of the complexes *cis*-[PdX₂(imzt)(PPh₃)] {imzt = imidazolidine-2-thione; PPh₃ = triphenylphosphine; X = Cl (1), Br (2), I (3), SCN (4)}, together with the effect of complexes 1–4 on the viability of U87MG human glioma cells.

Experimental

Instrumental

C, H and N analyses were performed by the Central Analítica at IQ—University of São Paulo, on a Perkin Elmer 2400 series II instrument. Conductivities were measured with a Digimed-DM-31 conductometer using 1×10^{-3} mol L⁻¹ solutions in DMF. IR spectra were recorded as KBr pellets on a Nicolet FTIR-Impact 400 spectrophotometer in the range

4000–400 cm⁻¹. ¹H NMR spectra were recorded in DMSO-*d*₆ solutions at room temperature on a Varian INOVA 500 spectrometer.

Synthesis

Dichlorido(imidazolidine-2-thione)(triphenylphosphine)palladium(II)·MeOH (1·MeOH): Complex 1·MeOH was prepared by adding a mixture of imidazolidine-2-thione (imzt) (40 mg; 0.39 mmol) and triphenylphosphine (101 mg; 0.39 mmol) in CHCl₃/CH₃OH (1:1, 4 mL) to an orange solution of [PdCl₂(CH₃CN)₂] (100 mg; 0.39 mmol) in CH₃OH (10 mL). After stirring the mixture for 1 h, the resulting suspension was filtered and the yellow solid was washed with methanol, chloroform and pentane and dried under vacuum. Yield: 77%.

Dibromido(imidazolidine-2-thione)(triphenylphosphine)palladium(II)·MeOH (2·MeOH): To a yellow suspension of [PdCl₂(imzt)(PPh₃)] (100 mg; 0.18 mmol) in MeOH (10 mL) was added a solution of KBr (44 mg, 0.37 mmol) in water (1 mL). After stirring the mixture for 6 h, the suspension was filtered and the brown solid was washed with water, methanol and dried under vacuum. Yield 82%.

Diiodido(imidazolidine-2-thione)(triphenylphosphine)palladium(II) (3): To a suspension of [PdCl₂(imzt)(PPh₃)] (100 mg; 0.18 mmol) in MeOH (10 mL) was added KI (61 mg, 0.37 mmol) in water (1 mL). After stirring for 1 h, the suspension was filtered and the brown solid was washed with water, methanol and dried under vacuum. Yield 93%.

Dithiocyanato(imidazolidine-2-thione)(triphenylphosphine)palladium(II) (4): To a suspension of [PdCl₂(imzt)(PPh₃)] (100 mg; 0.18 mmol) in MeOH (10 mL) was added a solution of KNCS (36 mg, 0.37 mmol) in water (1 mL). After stirring for 1 h, the suspension was filtered and the yellow solid was washed with water, methanol and dried under vacuum. Yield 95%.

Single-crystal X-ray diffraction studies

Single crystals for X-ray crystallography of 1·MeOH were obtained by slow evaporation of a solution of the complex from chloroform/methanol 1:1. Data collection was performed on a BRUKER KAPPA APEX II DUO diffractometer using graphite-monochromated MoK_α radiation ($\lambda = 0.71073$ Å) at 23 °C. The multi-scan absorption correction method was employed. SHELXS and SHELXL software were used for structure solution and refinement [20]. The hydrogen atom positions were refined with fixed individual isotropic displacement parameters using a riding model, except those bonded to the nitrogen and oxygen atoms, which were located in the Fourier difference map and refined with isotropic temperature parameters. All non-hydrogen atoms positions

were refined with anisotropic thermal displacements. Table 1 shows the crystallographic data and refinement conditions.

Cell culture and XTT assay

The U87MG human GBM (glioblastoma multiforme) cell line [American Type Culture Collection (ATCC)[®] HTB-14TM] was obtained from the ATCC (American Type Culture Collection, Manassas, VA, USA). Cells were cultured in Dulbecco's modified Eagle's medium (DMEM) Ham's F-10 (Sigma-Aldrich; Merck Millipore), supplemented with 10% fetal bovine serum (FBS; Cultilab, Campinas, Brazil) and 1% penicillin (10,000 units)/streptomycin (10 mg) (Sigma-Aldrich; Merck Millipore). Cells were incubated at 37 °C in an atmosphere containing 5% CO₂ until they reached semi-confluence, when they were used for proliferation experiments.

Test solutions of the compounds (1000 μM) were freshly prepared by dissolution in 50 μL of DMSO and

completed with 4950 μL of culture medium. These stock solutions were diluted in culture medium to reach final concentrations of 100, 50.0, 25.0, 12.5 e 6.25 μM. The DMSO solvent in the concentrations used did not reveal any cytotoxic activity compared to the untreated control. The average of how much DMSO interfered with the proliferation in comparison with the untreated control was 106.4 ± 22.3%.

For proliferation assay, GBM cells (5000 cells for 24 h and 500 cells for 120 h) were seeded in 96 well plates, cultured for 24 h and treated with the test compounds and the solvent control (DMSO) for 24 h. After PBS 1× washing, complete medium was added and cells were cultured for 24 or 120 h. After this incubation time, the medium was removed and cells were washed with PBS 1×. Cells were incubated for 2 h at 37 °C with 100 μL per well of a solution of XTT (sodium 3'-[1-(phenylaminocarbonyl)-3,4-tetrazolium]-bis(4-methoxy-6-nitro)benzene sulfonic acid hydrate) assay—Cell Proliferation Kit II—XTT, Roche Molecular Biochemicals) and DMEM without

Table 1 Crystal and structure refinement data for [PdCl₂(imzt)(PPh₃)]·CH₃OH (I·MeOH)

Formula	C ₂₂ H ₂₅ Cl ₂ N ₂ OPPdS
Formula weight	573.77
Wavelength	0.71073 Å
Crystal system	Monoclinic
Space group	P2 ₁ /c
Temperature (K)	296(2) K
<i>a</i> (Å)	12.9942(8)
<i>b</i> (Å)	9.7746(6)
<i>c</i> (Å)	20.1059(12)
β (°)	107.893(2)
<i>V</i> (Å ³)	2430.2(3)
<i>Z</i>	4
<i>D</i> _{calc}	1.568 Mg/m ³
Absorption coefficient	1.152 mm ⁻¹
<i>F</i> (000)	1160
Crystal size	0.960 × 0.630 × 0.270 mm ³
θ range for data collection (°)	1.647–26.405°
Index ranges	−16 ≤ <i>h</i> ≤ 16, −12 ≤ <i>k</i> ≤ 12, −25 ≤ <i>l</i> ≤ 25
Reflections collected	45,872
Independent reflections	4991 [<i>R</i> (int) = 0.0313]
Completeness to $\theta = 25.242^\circ$	100.0%
Absorption correction	Semi-empirical from equivalents
Max. and min. transmission	0.7454 and 0.5192
Refinement method	Full-matrix least-squares on <i>F</i> ²
Data/restraints/parameters	4991/0/284
Goodness-of-fit on <i>F</i> ²	1.069
Final <i>R</i> indices [<i>I</i> > 2σ(<i>I</i>)]	<i>R</i> 1 = 0.0215, <i>wR</i> 2 = 0.0519
<i>R</i> indices (all data)	<i>R</i> 1 = 0.0239, <i>wR</i> 2 = 0.0543
Largest diff. peak and hole	0.365 and −0.391 e Å ⁻³

phenol red (Sigma-Aldrich; Merck Millipore) supplemented with 10% FBS (Sigma-Aldrich; Merck Millipore) according to the manufacturer's protocol, followed by absorbance measurement (455 and 650 nm). Each experiment was performed in triplicate wells and repeated at least three times. The computer-based program GraphPad Prism was used to determine the IC₅₀ data.

Reaction with guanosine

The reaction with guanosine was carried out using the procedure described by Rocha et al. [16], with some modifications. Complex **1** (2.02 mg, 3.53 μmol) was dissolved in 0.2 mL of DMSO-*d*₆ in a microcentrifuge tube (1.5 mL). Then, AgNO₃ (1.20 mg, 7.06 μmol) was added and the mixture stirred for 10 min. The resulting white suspension was left to stand for 1 h at room temperature, then the insoluble solid was eliminated by centrifugation (14,000 rpm) to yield a yellow solution. A solution of guanosine (2.00 mg, 7.06 μmol) in DMSO-*d*₆ (0.2 mL) was added, and the solution was stirred for 10 min. The mixture was left to stand for 48 h before analysis by ¹H NMR spectroscopy.

Results and discussion

Chemistry

The precursor [PdCl₂(MeCN)₂] reacts with triphenylphosphine and imidazolidine-2-thione (imzt) in methanol to afford [PdCl₂(imzt)(PPh₃)]·MeOH (**1**·MeOH). The complexes [PdBr₂(imzt)(PPh₃)]·MeOH (**2**·MeOH), [PdI₂(imzt)(PPh₃)] (**3**) and [Pd(SCN)₂(imzt)(PPh₃)] (**4**) were readily obtained by metathesis of the chlorido ligands in **1** by bromide, iodide and thiocyanate salts, respectively. A general scheme which represents the strategy employed for the synthesis is illustrated in Scheme 1.

The complexes are air-stable powders and are yellow to brown in color. The molar conductivities of all four complexes in DMF are between 9.9 and 24.4 O⁻¹ cm² mol⁻¹, in agreement with their nonelectrolytic nature [21]. The complexes are soluble in DMF and DMSO, but insoluble in

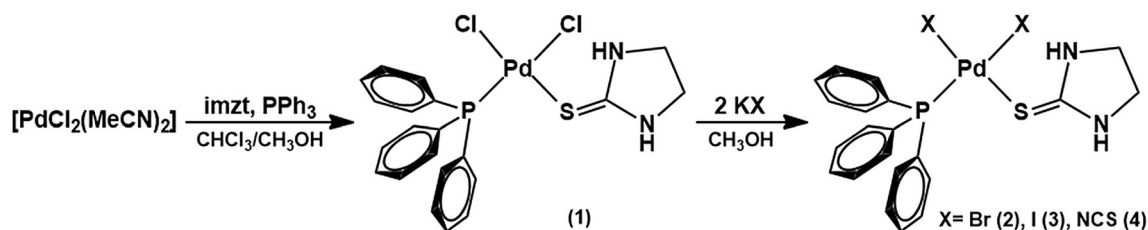
most other organic solvents. The elemental analyses were consistent with the empirical formulae C₂₂H₂₅Cl₂N₂OPPdS (**1**), C₂₂H₂₅Br₂N₂OPPdS (**2**), C₂₁H₂₁I₂N₂PPdS (**3**) and C₂₃H₂₁N₄PPdS₃ (**4**), agreeing well with their expected mononuclear compositions (Table 2).

Crystal structure of complex **1**

The crystal structure of **1**·MeOH has been determined by single-crystal X-ray diffraction, and its ORTEP representation with the atom labeling scheme is illustrated in Fig. 1. Selected interatomic bond distances and angles with their estimated standard deviations are shown in Table 3.

Complex **1** crystallizes in the monoclinic space group P2₁/c, with the asymmetric unit being constituted by one complex molecule and one methanol solvate molecule. The palladium(II) center is coordinated by two *cis*-positioned chlorido ligands, one imidazolidine-2-thione and one triphenylphosphine ligand (Fig. 1). The observed *cis* configuration is the expected result of the mutual destabilizing effects of phosphorus and sulfur ligands in *trans* positions when coordinated to a class *b* metal center (antisymbiotic effect) [22]. The geometry around Pd^{II} is essentially square planar, with interatomic bond angles that deviate slightly from 90° (S1–Pd1–Cl2 = 92.80(2)°, P1–Pd1–Cl1 = 92.06(2)°, Cl1–Pd1–Cl2 = 89.43(2)°, S1–Pd1–P1 = 85.88(2)°). The Pd1–Cl1 and Pd1–Cl2 bond lengths agree well with those observed in other Pd^{II} compounds [17]. Nevertheless, the two Pd–Cl bond distances were found to be distinct: The shorter Pd1–Cl1 (2.3026(5) Å) is located *trans* to the S1 atom, whereas the longer Pd1–Cl2 (2.3958(5) Å) is *trans* to the P1 atom. This finding is associated with the different *trans* influences of the triphenylphosphine and imidazolidine-2-thione ligands. The Pd1–S1 (2.3169(5) Å) and Pd1–P1 (2.2554(5) Å) distances are comparable to those found in the complex *cis*-[PdCl₂(tu)(PPh₃)] (tu = thiourea) [17] at 2.3191(1) and 2.2440(1) Å, respectively.

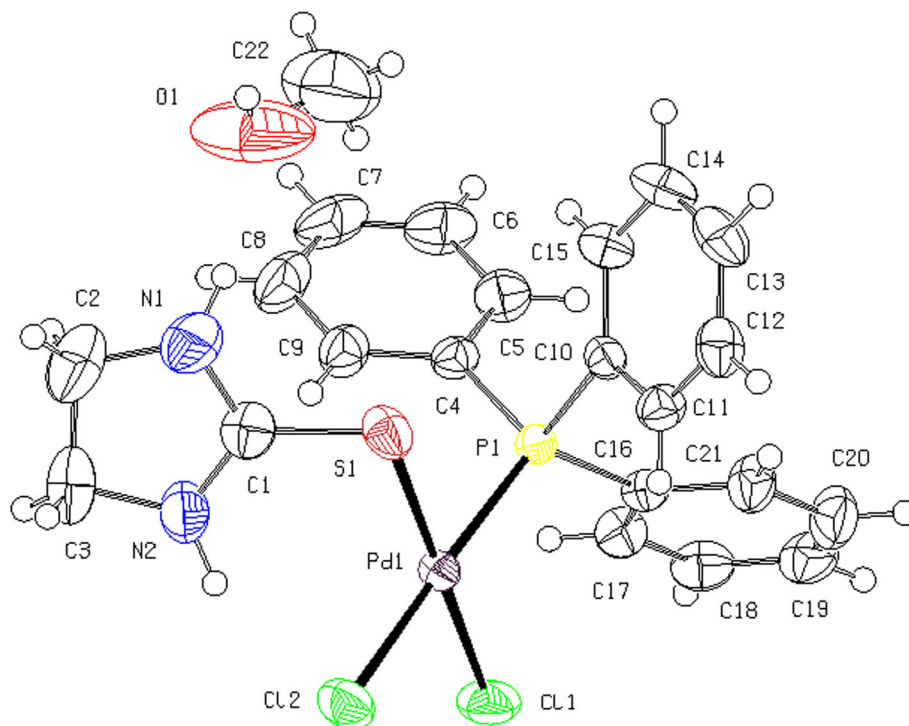
Upon coordination, modifications of the bond distances of the thiourea moiety in the imidazolidine-2-thione ligand are observed. According to crystallographic studies on free imidazolidine-2-thione [23], the CS and CN bonds are 1.692(1) and 1.328 (mean) Å. The significant lengthening



Scheme 1 Synthesis of complexes **1–4**

Table 2 Analytical and physicochemical data for the complexes

Complex	Λ_M ($\Omega^{-1} \text{ cm}^2 \text{ mol}^{-1}$)	M.p. ($^{\circ}\text{C}$)	Carbon		Nitrogen		Hydrogen	
			Found (%)	Calc. (%)	Found (%)	Calc. (%)	Found (%)	Calc. (%)
$\text{C}_{22}\text{H}_{25}\text{Cl}_2\text{N}_2\text{OPPdS}$ (1 ·MeOH)	10.6	162	46.00	46.05	4.82	4.88	4.28	4.39
$\text{C}_{22}\text{H}_{25}\text{Br}_2\text{N}_2\text{OPPdS}$ (2 ·MeOH)	15.2	138	39.90	39.87	4.34	4.23	3.62	3.80
$\text{C}_{21}\text{H}_{21}\text{I}_2\text{N}_2\text{PPdS}$ (3)	24.4	132	35.02	34.81	3.76	3.87	3.05	2.92
$\text{C}_{23}\text{H}_{21}\text{N}_4\text{PPdS}_3$ (4)	9.9	191	47.16	47.06	9.56	9.54	3.73	3.61

Fig. 1 ORTEP representation of *cis*-[PdCl₂(imzt)(PPh₃)]·CH₃OH (**1**·MeOH), showing the labeling of the atoms. Displacement ellipsoids are drawn at the 50% probability level**Table 3** Selected geometric parameters (\AA , $^{\circ}$) for *cis*-[PdCl₂(imzt)(PPh₃)]·MeOH (**1**·MeOH)

Bond distances		Bond angles	
Pd1–S1	2.3169(5)	S1–Pd1–P1	85.88(2)
Pd1–P1	2.2554(5)	S1–Pd1–Cl1	176.76(2)
Pd1–Cl1	2.3026(5)	S1–Pd1–Cl2	92.80(2)
Pd1–Cl2	2.3958(5)	P1–Pd1–Cl1	92.06(2)
		P1–Pd1–Cl2	175.92(2)
		Cl1–Pd1–Cl2	89.43(2)

of the C(1)–S(1) distance (from 1.692(1) to 1.724(2) \AA) together with a shortening of C(1)–N(1) and C(1)–N(2) bond lengths (from 1.328 to 1.319(3) and 1.321(3), respectively) clearly indicates changes in the electron density distribution. Hence the CS bond is weakened, while

the π -bond character of the CN bonds is strengthened upon complexation. Such behavior has already been observed in other metal-based complexes of imidazolidine–thiones [24].

The crystal packing is stabilized by several hydrogen bonds (see Table S5, Sup. Mat.) in which the NH groups of imzt take part in intramolecular and intermolecular interactions of the type N(2)–H(2)···Cl(2) and N(1)–H(1)···O(1), respectively. The methanol solvate also participates in intermolecular hydrogen bonds of the type O(1)–H(1S)···Cl(2)^{−x,y−1/2,−z+1/2} with O(1)···Cl(2) distance of 3.192(3) \AA .

Spectroscopic studies

The most significant IR data for free imzt and its palladium(II) complexes **1–4** are summarized in Table 4.

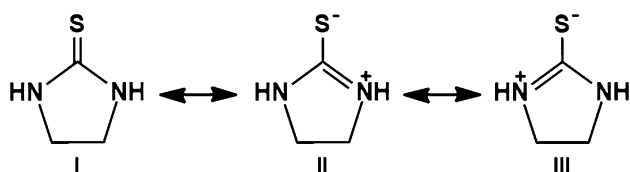
Table 4 Selected vibrational data (cm^{-1}) for the complexes and free ligands

imzt ^a	PPh ₃ ^b	1-MeOH	2-MeOH	3	4	Assignment
3246 s	–	3439 m	3437 m	–	–	$\nu\text{OH}_{\text{methanol}}$
–	–	3363 sh	3363 m	3361 s	–	νNH
–	–	3207 m	3180 sh	3174 sh	3180 ms	νNH
–	–	3140 m	3133 m	3132 s	–	νNH
–	3054 m	3050 m	3052 w	^c	3052 w	νCH (PPh ₃)
2883 s	–	2892 m	2890 mw	2887 mw	2898 mw	$\nu_{\text{as}}\text{CH}_2$
–	–	–	–	–	2107 s	$\nu_{\text{as}}\text{SCN}$
1522 s	–	1536 s	1535 s	1535 s	1533 s	$\nu\text{CN} + \delta\text{NH}$
–	1482 s	1479 m	1480 m	1480 s	1481 m	ν_{ring} (PPh ₃)
–	1435 s	1435 s	1435 m	1435 s	1435 m	ν_{ring} (PPh ₃)
–	1322 w	1324 m	1320 m	1315 m	1312 m	ν_{ring} (PPh ₃)
–	1089 m	1095 m	1096 m	1094 m	1095 m	X-sensitive mode <i>q</i> (PPh ₃)
925 mw	–	914 w	915 w	916 w	915 w	$\nu_{\text{ring}} + \nu\text{CS} + \nu\text{CN}$
–	746 s	752 m	753 m	745 m	747 m	γCH (PPh ₃)
–	692 s	694 m	694 m	692 s	691 s	γ_{ring} (PPh ₃)
–	512 s	532 s	533 s	517 s	527 s	X-sensitive mode <i>y</i> (PPh ₃)
516 s	–	^c	^c	^c	^c	$\nu\text{CS} + \gamma_{\text{ring}}$
–	497 s	510 s	511 m	^c	509 s	X-sensitive mode <i>y</i> (PPh ₃)
–	489 s	496 s	497 s	503 s	494 s	X-sensitive mode <i>y</i> (PPh ₃)

Intensity: *s* strong, *ms* medium-strong, *m* medium, *w* weak, *sh* shoulder^a Ref. [26], ^b Ref. [27], ^c masked

IR spectroscopy is one of the most widely used spectroscopic techniques to assign the coordination mode of imidazolidine-2-thione ligands. According to Wheatley [25], the electronic structure of imidazolidine-2-thione may be denoted by a hybrid of three canonical forms (I, II and III), as shown in Scheme 2.

The IR spectrum of imidazolidine-2-thione has been reported previously, and key absorption bands have been assigned [26]. In principle, imzt can coordinate through both sulfur and nitrogen atoms. Upon *S*-coordination, the contribution of the structures II and III will be enhanced, leading to weakening of the CS bond. According to Dwarakanath and Sathyanarayana [26], the bands at 516 and 925 cm^{-1} in free imzt possess considerable $\nu\text{C}=\text{S}$ contribution. Thus, the shift of these absorptions to lower frequency on coordination is characteristic of the *S*-coordination mode. On the other hand, the νCN band (1509 cm^{-1} in free imzt) shifts to higher frequencies because of the greater double bond character of the CN bond on *S*-coordination. In the present case, the

**Scheme 2** Resonance forms of imidazolidine-2-thione

coordination of imzt via the thione sulfur is suggested by the shift to higher frequency of the νCN band from 1509 cm^{-1} to ca. 1535 cm^{-1} (1–4), while the thione group band is red shifted from 925 cm^{-1} to ca. 915 cm^{-1} (1–4). The other band with the highest νCS contribution was masked by the strong absorptions of triphenylphosphine over the 520–400 cm^{-1} spectral range [16, 27]. The coordination of neutral imzt in 1–4 is clearly evidenced by the presence of intense νNH absorptions between 3380 and 3120 cm^{-1} . In particular, the IR spectra of the halido-complexes 1–3 share a common feature in this spectral range; the presence of a sharp band at $\sim 3363 \text{ cm}^{-1}$ and two overlapped absorptions at ca. 3180 and 3130 cm^{-1} . This is attributed to involvement of the imzt NH groups in different types of hydrogen bonding [28]. The similar patterns observed for the νNH bands suggest that the complexes 1–3 have closely related structures. The IR spectrum of complex 4 exhibits a single broad νNH absorption at 3180 cm^{-1} , indicating that the polynuclear nature of the anionic ligand gives rise to a distinct hydrogen bonding network. For complex 4, the observation of a relatively broad and intense $\nu_{\text{as}}\text{SCN}$ band at 2104 cm^{-1} supports the terminal *N*-bonded coordination mode for the thiocyanato ligand [29]. The presence of methanol solvate in 1 and 2 was detected by a typical νOH absorption at ca. 3448 cm^{-1} .

The low solubilities of the complexes were sufficient for their conductivity values and ^1H NMR spectra to be

measured, but their ^{13}C NMR spectra could not be recorded. The insolubility of complex **3** in all common deuterated solvents hindered us from obtaining its NMR spectrum. However, ^1H NMR spectroscopy also unequivocally allowed assignment of the *S*-coordination mode of the imzt ligand in complexes **1**, **2** and **4**. Chemical shifts and assignment are summarized in Table 5.

Significant shifts are observed for the NH and $-\text{CH}_2-$ resonances in the complexes. The NH resonance changed from 7.95 ppm (free imzt) to ca. 8.8 ppm (complexes), whereas the $-\text{CH}_2-$ signal was displaced by ca. 0.4 ppm to downfield. This shift is assigned to the delocalization of π -electrons between N atoms as a consequence of the greater double bond character of the CN bond, as well as the weakening of the CS bond on complex formation [30]. Such spectroscopic behavior agrees well with the crystallographic results for complex **1**, which showed changes in the bond lengths of the “HNC(S)NH” moiety upon complexation. In addition, the presence of an N–H signal in the ^1H NMR spectra indicated that the imzt ligands are coordinated in the thione form in solution [31]. Integration of the proton signals was in accordance with the requirements for **1**, **2** and **4**. A signal at 3.15 ppm in the spectra of **1** and **2** is attributed to the methyl group of the MeOH molecule. In agreement with the

analytical and spectroscopic data together with the crystallographic results on complex **1**, a proposal for the structures of the analogous compounds **2**·MeOH, **3** and **4** has been suggested, in which the metal center is coordinated to two anions {bromido (**2**·MeOH), iodido (**3**) or *N*-thiocyanato (**4**)}, one imidazolidine-2-thione ligand, and one triphenylphosphine ligand in a *cis* configuration (Scheme 1).

Cytotoxic activities against human glioblastoma

The cytotoxic activities of the free PPh_3 , imzt and the palladium(II) complexes have been evaluated against human glioblastoma cell line (U87MG). Cells were exposed to a range of Pd^{II} complex concentrations (100, 50, 25, 12.5 and 6.25 μM) for 24 h (Fig. 2) and 120 h (Fig. 3).

As shown in Fig. 2, after 24 h of incubation, concentrations of 10–50 μM of all four complexes did not modify the viability of the U87MG cell line. However, the number of viable cells for complex **1** was reduced to 50% at $69.65 \pm 1.04 \mu\text{M}$, while complexes **2** and **4** were much less active in this concentration. Complex **3** was considered to be inactive at all tested concentrations.

After 120 h of exposure (Fig. 3), complex **1** exhibited the highest cytotoxic effect ($\text{IC}_{50} = 56.01 \pm 1.06 \mu\text{M}$),

Table 5 ^1H NMR data for imzt and complexes **1**, **2** and **4** at 298 K, in $\text{DMSO}-d_6$, given as ppm, multiplicity, [integration]

Nuclei	imzt	1	2	4
<i>^1H-NMR</i>				
NH	2.17 s, [2H]	8.79 s, [2H]	8.82 s, [2H]	8.90 s, [2H]
$-\text{CH}_2-$	6.18 s, [4H]	3.49 s, [4H]	3.49 s, [4H]	3.50 s, [4H]
PPh_3	–	7.70–7.45 m [18 H]	7.69–7.46 m [18 H]	7.72–7.48 m [18 H]

s singlet, *m* multiplet

Fig. 2 Viability of U87MG (% of control) after 24-h incubation with complexes **1–4**

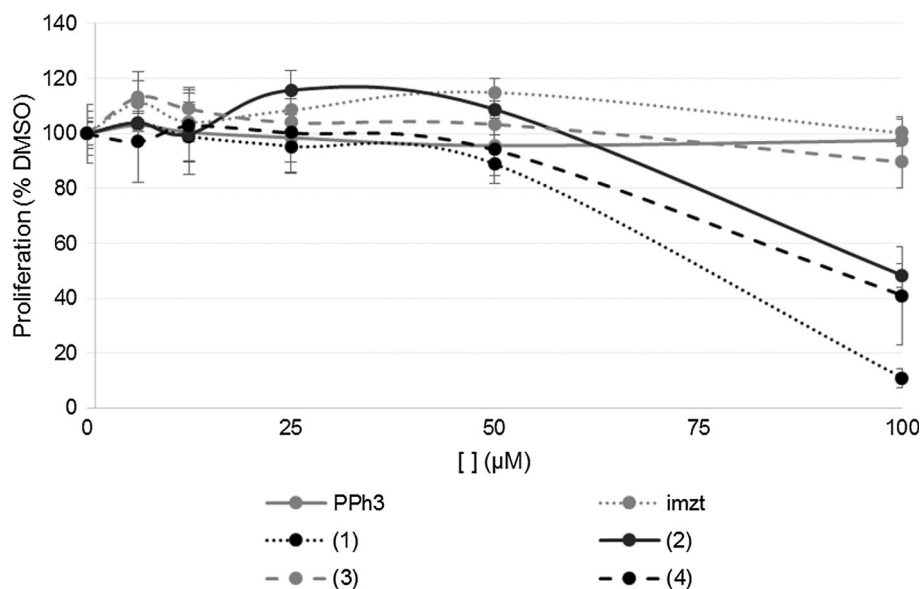
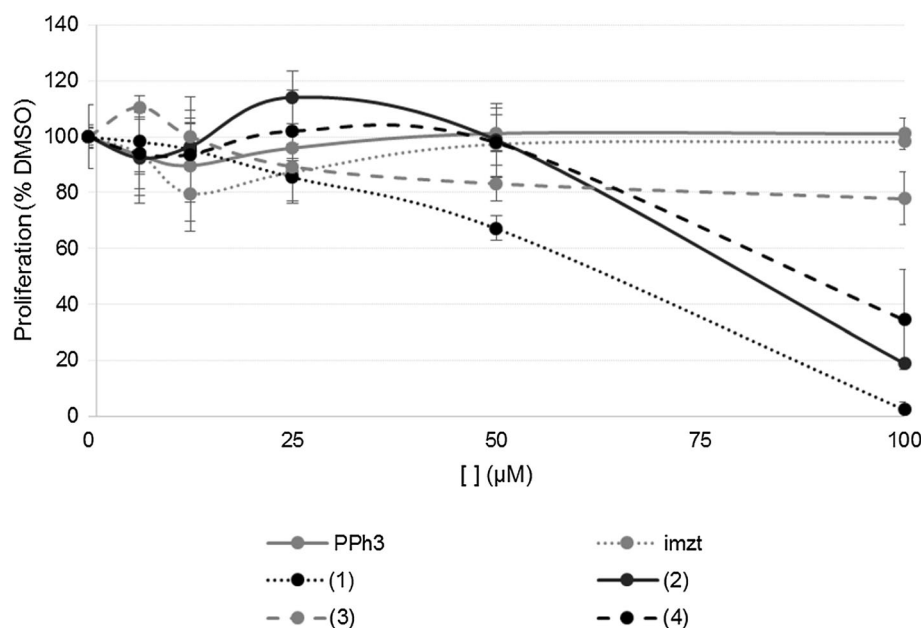


Fig. 3 Viability of U87MG (% of control) after 120-h incubation with complexes 1–4



whereas **2** and **4** were able to reduce the number of viable U87MG cells to 50% at concentrations of 86.59 ± 0.16 and 95.08 ± 1.07 μM , respectively.

The 50% inhibitory concentration values obtained for the complexes **1–4** after 24 and 120 h incubation times are summarized in Table 6.

Complex **1** reduced the viability of U87MG tumor cells over time at concentrations as low as 100 μM . This effect was observed within 24 h of treatment and persisted for over 120 h. It is important to emphasize that complex **1** was much more active against U87MG tumor cells than temozolomide (TMZ), the first line drug employed in the treatment of brain cancer [32]. After 24 h of exposure, TMZ had not demonstrated any cytotoxic effect, even at high drug concentrations (1000 μM). On the other hand, 120 h of exposure was sufficient to reduce to 50% the number of viable cells at 200 μM of TMZ [32]. These findings indicate that complex **1** is more active than TMZ *in vitro* after 24 and 120 h incubation times.

The cytotoxicity data reveal an interesting trend, in that the cytotoxicity level of the complexes decreased according to the anionic ligand X, following the order $\text{Cl} > \text{Br} \approx \text{SCN} \gg \text{I}$, which implies that the lability of the Pd–X bond may be playing a key role in determining the activities of these compounds. Taking into account that the free ligands are inactive, the mode of action of the most active chlorido-complex may involve the initial transportation of $[\text{PdCl}_2(\text{imzt})(\text{PPh}_3)]$ into the tumor cells, followed by reaction (of the complex or one of its hydrolysis products) at the active sites. In line with this hypothesis, it is well-established that *cis*-dichlorido Pd(II) complexes interact with DNA in an analogous manner to their Pt(II) counterparts

[18]. Hence, in order to gain more knowledge about its reactivity toward DNA, we have evaluated the ability of complex **1** to bind to guanosine, a model for a purine base.

Interaction of complex 1 with guanosine

It is well known that the antitumor activity of various platinum-based pharmaceuticals is associated with their platination of DNA, most commonly through binding to guanine. Similarly to cisplatin, some palladium(II) compounds can also coordinate to N7 of guanine [33]. We have therefore selected guanosine as a purine model system to study the reactivity of complex **1** by means of ^1H NMR spectroscopy.

The reaction between guanosine and **1** was initially studied in DMSO because of the low solubility of the

Table 6 Cytotoxicity data (IC_{50}) of free imzt and PPh_3 and complexes **1–4** against U87MG tumor cells after 24- and 120-h incubation times

Compound	IC_{50} (μM) \pm SD	
	24 h	120 h
1	69.65 ± 1.04	56.01 ± 1.06
2	99.75 ± 1.6	86.59 ± 0.16
3	>100	>100
4	99.49 ± 1.04	95.08 ± 1.07
PPh_3	a	a
imzt	a	a
TMZ ^b	>1000	200

^a Ligands did not show a dose–response pattern, ^b Ref. [32]

complex in aqueous media. However, complex **1** did not react with guanosine after 48 h under such conditions. Therefore, to enhance reactivity, chlorido abstraction of **1** by silver nitrate in DMSO was undertaken, affording a reactive nitrate/solvento complex in situ. Thus, a solution of complex **1** in DMSO- d_6 was left to react for 1 h with two equivalents of AgNO_3 , then the insoluble AgCl was eliminated by centrifugation. The resulting yellow solution

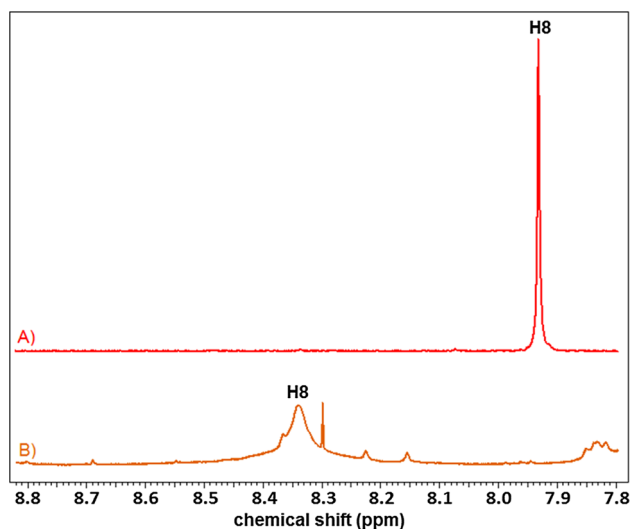
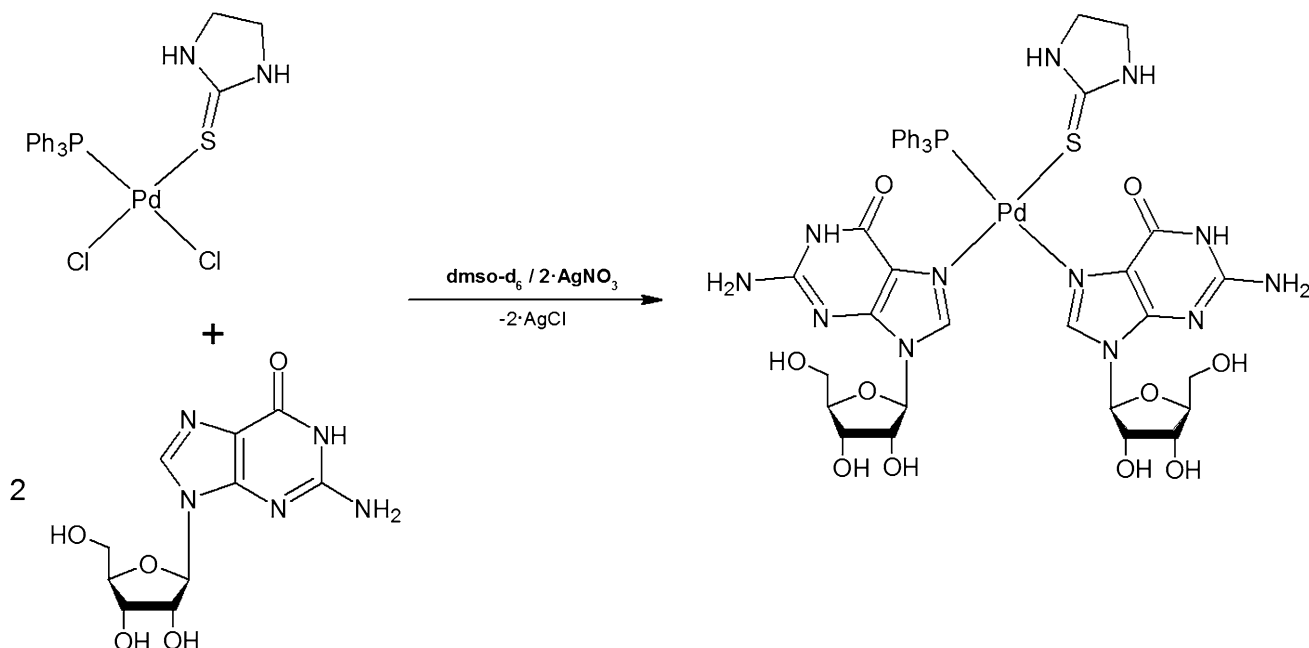


Fig. 4 *a* ^1H NMR spectrum of guanosine in DMSO- d_6 in the 8.8–7.8 range; *b* ^1H NMR spectrum of complex **1**, treated with AgNO_3 followed by guanosine



Scheme 3 Reaction of complex **1** pretreated with AgNO_3 with guanosine

was mixed with guanosine (2.0 eq.) and left to stand for 48 h before being analyzed by ^1H NMR spectroscopy. Under these conditions, the nitrate/solvento complex reacted with guanosine, yielding an adduct with molar ratio 1:2 palladium(II)–guanosine. A downfield shift (0.41 ppm) of the signal attributed to the H8 atom from guanosine (Fig. 4) is characteristic of metal coordination via N7 [34] (Scheme 3).

We conclude that complex **1** is capable of interacting with guanosine only after the removal of its chlorido ligands by AgNO_3 . It is important to point out that the limited reactivity of **1** with guanosine is not enough to rule out the involvement of DNA as a molecular target. Nevertheless, there is a growing body of evidence that suggests that palladium(II) compounds exert their activity by different mechanisms than those observed for classical platinum(II) complexes. In this context, Rocha et al. [12] reported that complexes of the type $[\text{PdX}(\text{PPh}_3)_2(\text{4-MeT})]\text{X}$ { PPh_3 = triphenylphosphine; 4-MeT = 4-methyl-3-thiosemicarbazide; $\text{X} = \text{Cl}, \text{Br}, \text{I}, \text{SCN}$ } displayed a scarce reactivity toward DNA, but were capable of inhibiting human topoisomerase II α and cathepsin B at a micromolar concentration range. Another interesting example involving a phosphine-based palladium(II) complex was described by Gigli et al. [35]. In this work, the death of melanoma cells induced by $[\text{Pd}_2(\text{S}_C\text{-C}^2\text{-N-dmpa})_2(\mu\text{-dppf})\text{Cl}_2]$ (dmpa = *N,N*-dimethyl-1-phenethylamine; dppf = 1,2-bis(diphenylphosphino)ferrocene) involved the lysosomal-mitochondrial axis, being characterized by

lysosomal membrane permeabilization, cathepsin B activation and increased Bax protein levels following its translocation to mitochondria [35]. In addition, some palladium(II) compounds, in contrast to their platinum(II) analogs, have been found to be non-mutagenic in the Ames test [19].

Conclusions

In conclusion, we have successfully prepared and characterized four new palladium(II) complexes. All four complexes are assigned a *cis* configuration, as a result of the antisymbiotic effects of the triphenylphosphine and imidazolidine-2-thione ligands. In all four complexes, the imzt acts as an *S*-monodentate ligand. The fact that complex **1** displayed higher cytotoxicity than its analogs suggests that changing halido or pseudohalido ligands (X) exerts an effect on the cytotoxicity of this class of compounds. Currently ongoing studies in our laboratories are aiming at rationalizing the cytotoxicity in terms of structure-activity relationships.

Supplementary data

CCDC 1538112 contains the supplementary crystallographic data for **1**-MeOH. These data can be obtained free of charge via <http://www.ccdc.cam.ac.uk/conts/retrieving.html>, or from the Cambridge Crystallographic Data Centre, 12 Union Road, Cambridge CB2 1EZ, UK; fax: (+44) 1223-336-033; or e-mail: deposit@ccdc.cam.ac.uk.

Acknowledgements This work was sponsored by Grants from FAPESP (proc. 2009/54011-8, 2012/15486-3 and 2016/17711-5), FAPEMIG, CNPq (proc. 475322/2009-6 and 422105/2016-3) and CAPES.

References

- Louis DN, Ohgaki H, Wiestler OD, Cavenee WK, Burger PC, Jouvot A, Scheithauer BW, Kleihues P (2007) *Acta Neuropathol* 114(2):97–109
- Stupp R, Hegi ME, van den Bent MJ, Mason WP, Weller M, Mirimanoff RO, Cairncross JG (2006) *Oncologist* 11:165–180
- Stupp R, Mason WP, van den Bent MJ, Weller M, Fisher B, Taphoorn MJ, Belanger K, Brandes AA, Marosi C, Bogdahn U, Curschmann J, Janzer RC, Ludwin SK, Gorlia T, Allgeier A, Lacombe D, Cairncross JG, Eisenhauer E, Mirimanoff RO (2005) *N Engl J Med* 352:987–996
- Warnick RE, Prados MD, Mack EE, Chandler KL, Doz F, Rabbitt JE, Malec MK (1994) *J Neurooncol* 19(1):69–74
- Roci E, Cakani B, Brace G, Bushati T, Rroji A (2014) *Med Arch* 68(2):140–143
- Wang D, Lippard SJ (2005) *Nat Rev Drug Discov* 4(4):307–320
- Medici S, Peana M, Nurchi VM, Lachowicz JI, Crisponi G, Zoroddu MA (2015) *Coord Chem Rev* 284(1):329–350
- Garoufils A, Hadjidakou SK, Hadjiliadis N (2009) *Coord Chem Rev* 253:1384–1397
- Ramos-Lima FJ, Quiroga AG, Garcia-Serrelde B, Blanco F, Carnero A, Navarro-Ranninger C (2007) *J Med Chem* 50(9):2194–2199
- Caires ACF, Almeida ET, Mauro AE, Hemerly JP, Valentini SR (1999) *Quim Nova* 22(3):329–334
- Nadeem S, Bolte M, Ahmad S, Fazeelat T, Tirmizi SA, Rauf MK, Sattar SA, Siddiq S, Hameed A, Haider SZ (2010) *Inorg Chim Acta* 363:3261–3269
- Rocha FV, Barra CV, Garrido SS, Manente FA, Carlos IZ, Ellena J, Fuentes ASC, Gautier A, Morel L, Mauro AE, Netto AVG (2016) *J Inorg Biochem* 159:165–168
- Barra CV, Rocha FV, Morel L, Gautier A, Garrido SS, Mauro AE, Frem RCG, Netto AVG (2016) *Inorg Chim Acta* 446:54–60
- Legendre AO, Mauro AE, Ferreira JG, Ananias SR, Santos RHA, Netto AVG (2007) *Inorg Chem Commun* 10:815–820
- Netto AVG, Frem RCG, Mauro AE (2001) *Mol Cryst Liq Cryst* 374:255–260
- Rocha FV, Barra CV, Mauro AE, Carlos IZ, Nauton L, Ghoszi ME, Gautier A, Morel L, Netto AVG (2013) *Eur J Inorg Chem* 25:4499–4505
- Moro AC, Watanabe FW, Ananias SR, Mauro AE, Netto AVG, Lima APR, Ferreira JG, Santos RHA (2006) *Inorg Chem Commun* 9:493–496
- Barra CV, Rocha FV, Gautier A, Morel L, Quilles MB, Carlos IZ, Treu-Filho O, Frem RCG, Mauro AE, Netto AVG (2013) *Polyhedron* 65:214–220
- Moro AC, Cunha GA, Souza RFF, Mauro AE, Netto AVG, Carlos IZ, Resende FA, Varanda EA, Pavan FR, Leite CQF (2015) *Med Chem Res* 24:2879–2888
- Sheldrick GM (2008) *Acta Cryst A* 68:112–122
- Geary WJ (1971) *Coord Chem Rev* 7:81–122
- Pearson RG (1973) *Inorg Chem* 12(3):712–713
- Mak TW, Jasim KS, Chieh C (1984) *Can J Chem* 62:808
- Raper ES, Creighton JR, Wilson JD, Clegg W, Milne A (1989) *Inorg Chim Acta* 155:85–89
- Wheatley PJ (1953) *Acta Cryst* 6:369–377
- Dwarakanath K, Sathyanarayana DN (1979) *Bull Chem Soc Jpn* 52:2699–2704
- Deacon GB, Green JHS (1967) *Spectrochim Acta A* 24:845–852
- Bowmaker GA, Chaichit N, Pakawatchai C, Skelton BW, White AH (2009) *Can J Chem* 87:161–170
- Burmeister JL, Basolo F (1964) *Inorg Chem* 3:1587–1593
- Ashraf W, Ahmad S, Isab AA (2004) *Transit Metal Chem* 29:400–404
- Wazeer MIM, Isab AA (2007) *Spectrochim Acta A* 68:1207–1212
- Montaldi AP, Sakamoto-Hojo ET (2013) *Clin Exp Med* 13:279–288
- Barnham KJ, Bauer CJ, Djuran MI, Mazid MA, Rau T, Sadler PJ (1995) *Inorg Chem* 34:2826–2832
- Chevry A, Teyssot ML, Maisonia A, Lemoine P, Viossat B, Traïkia M, Aitken DJ, Alves G, Morel L, Nauton L, Gautier A (2010) *Eur J Inorg Chem* 22:3513–3519
- Gigli R, Pereira GJS, Antunes F, Bechara A, Garcia DM, Spindola DG, Jasiulionis MG, Caires ACF, Smaili SS, Bincoletto C (2016) *Eur J Med Chem* 107:245–254